



University of Pennsylvania School of Dental Medicine

¹⁸F-FDG-PET/CT in Radiation Therapy-Induced Parotid Gland Inflammation

Alaa Mouminah, BDS

A THESIS

Presented to the Faculty of Penn Dental Medicine in Fulfillment of the Requirements for the
Degree of Master of Oral Biology

2020

Thesis Committee

Abass Alavi

Abass Alavi, MD, PhD, DSc
Department of Radiology
University of Pennsylvania

M-E Revheim

Mona-Elisabeth Revheim, MD, PhD
Division of Radiology and Nuclear Medicine

Jonathan Korostoff, DMD, PhD
Department of Periodontics
University of Pennsylvania
School of Dental Medicine

Yu Cheng Chang, DDS, MS, DMD
Department of Periodontics

ABSTRACT

Background

¹⁸F-fluorodeoxyglucose-positron emission tomography/computed tomography (FDG-PET/CT) is used in the clinical management of oncologic and inflammatory pathologies. It may have utility in detecting radiotherapy (RT)-induced damage of oral tissues. Thus, the aim of the present study was to use FDG-PET/CT to evaluate parotid gland inflammation following RT in patients with head and neck cancer (HNC).

Methods

This retrospective study included patients with HNC treated with photon, proton, or combined photon/proton RT, in addition to chemotherapy. All patients received FDG-PET/CT imaging pre-treatment and 3 months post-treatment. The average mean standardized uptake value (Avg SUVmean) and the average maximum standardized uptake value (Avg SUVmax) of the left and right parotid glands were determined by global assessment of FDG activity using OsiriX MD software. A two-tailed paired t-test was used to compare Avg SUVmean and Avg SUVmax pre- and post-RT.

Results

Forty-seven HNC patients were included in the study. Parotid gland Avg SUVmean was significantly higher at 3 months post-treatment than pre-treatment ($p<0.05$) in patients treated with photon RT, but no significant differences were found between pre- and post-treatment Avg SUVmean in patients treated with proton RT or combined photon/proton RT.

Conclusion

Our results suggest that photon RT may cause radiation-induced inflammation of the parotid gland, and that proton RT, which distributes less off-target radiation, is a safer treatment alternative.

Keywords: PET/CT, 18F-FDG, Radiation therapy, Parotid gland, Parotid gland inflammation, Head and neck cancer

INTRODUCTION

Head and neck cancers (HNC) represent about 4% of all cancers in the United States [1]. This group of malignancies affect a variety of anatomic structures, including the oral cavity, oropharynx, nasopharynx, hypopharynx, larynx, paranasal sinuses, and salivary glands [2]. Along with surgical resection and/or chemotherapy, HNC may be treated with radiation therapy (RT) as either definitive or adjuvant treatment [2].

The majority of radiation treatment modalities for HNC consist of external beam photon therapy, which has been associated with many systemic sequelae including pneumonitis and vasculitis [3,4]. Oral complications of RT have proven to be very common in cancer patients, especially those with HNC [5]. Critical anatomical structures in close proximity to the irradiated area are often affected during treatment resulting in complications including fibrosis, taste changes, dental caries, periodontal disease, and oral mucositis [2,6]. Because these alterations can have adverse effects on the lifestyle and health outcomes of HNC patients, it is critical to establish an understanding of the off-target effects of RT on the oral region which contains tissues that are particularly susceptible to radiation-induced damage.

The parotid gland is the largest of the salivary glands and produces 60% to 65% of the total saliva in the oral cavity. It is wrapped around the ramus of the mandible in humans and may be an unintentional target in RT for HNC. Inflammation of the parotid gland has been demonstrated to induce xerostomia resulting in dryness of the oral cavity [7,8]. Of

note, radiation-induced xerostomia is the most frequently reported complications of RT for HNC and significantly affects HNC patients' quality of life [9].

Traditional imaging modalities such as computed tomography (CT) and magnetic resonance imaging (MRI) have been used for staging and monitoring structural changes. In contrast, positron emission tomography (PET) is frequently used to visualize physiological and molecular changes [10]. ^{18}F -fluorodeoxyglucose (FDG) is the most commonly used tracer for PET scanning. It is a radiolabeled glucose analog, taken up by cells that rapidly consume and metabolize glucose, such as cancer and inflammatory cells [11–13]. The fused FDG-PET/CT allows for detection and quantification of glucose metabolism on the molecular level leading to a more accurate detection of malignancies and inflammatory changes in the head and neck [14,15] .

LITERATURE REVIEW

Proton Radiotherapy is a specialized technique that is not available to a large number of patients. As proton radiotherapy becomes more accessible, studies reporting clinical outcomes are becoming steadily important. The maximum dose of photons are near the surface followed by a continuous reduction in dose with depth. This physical advantage of protons over photons is highly important. On the other hand, proton beam energies can produce a spread out that covers the tumor accurately and delivers a lower dose to normal tissues beyond the tumor. These features allow for better target dose delivery than photon techniques.

In a nonrandomized retrospective study by Baumann et al. they compared the effectiveness of proton versus photon in HNC patients. The study included 1483 adult patients with locally HNC advanced cancer treated with chemoradiotherapy and received proton or photon therapy. The objective was to assess whether proton therapy is associated with fewer unplanned hospitalizations or other adverse events and similar disease-free and overall survival compared with photon therapy. In this analysis, they concluded that proton chemoradiotherapy was associated with significantly reduced acute adverse events that caused unplanned hospitalizations, with similar disease-free and overall survival.[16]

As our main focus is salivary glands, this study conducted by Grant et al. is the only study reporting on outcomes for salivary gland tumors but in the pediatric population comparing proton versus photon radiotherapy. They retrospectively analyzed 24 cases of pediatric salivary gland tumors and found that proton therapy was associated with a favorable acute toxicity. When they compared proton to conventional radiotherapy, they detected that patients who received proton therapy experienced significantly less acute mucositis and a trend toward significantly less dysphagia and weight loss. Also, proton therapy was associated with reduced dose to several surrounding normal structures relative to photon therapy. In this study of pediatric salivary tumors, they revealed that proton therapy is associated with favorable outcomes. This finding highlights the advantage of proton therapy, which is in reduced exit but not entrance dose.[17]

A systematic review was performed to retrieve evidence on late treatment toxicity for carbon-ion, proton and photon radiotherapy. They included eight comparative studies

and 86 observational studies. Although poorly reported, toxicity tended to be less frequent in carbon-ion and proton studies compared to photons. No late xerostomia or dysphagia were observed in proton radiotherapy related results. Protons can be used to deliver a lower normal tissue dose while keeping the target dose similar, so the control of the tumor is anticipated to be similar to the results of photon radiotherapy. There is a strong depended relation between the severity of radiation-induced side effects and the dose and volume of the radiation area, where it will likely be less in proton radiotherapy.[18]

Much of the existing literature on the clinical application of FDG has focused on the radiotracer's utility in diagnosing malignancies due to the typically increased glucose metabolism of cancer cells, but FDG has also been used for decades to detect inflammatory processes. Therefore, we predict that FDG-PET/CT will show potential in the evaluation of radiation-induced inflammation in the parotid gland that predisposes patients to xerostomia.

A retrospective study by Roach et al. in patients with head and neck squamous cell carcinoma (HNSCC) aimed to identify the relationship of radiation dose response of parotid gland glucose metabolism. They used the same technique we are proposing in our present study, but the pretreatment and post treatment scans varied between 3 and 6 months. They aimed to identify a threshold radiation dose where the parotid gland activity declined. The mean dose threshold in this study was 32 Gray.[19]

As we discussed previously, most of the existing literature aims to identify the radiation dose– response relationship of parotid gland in head and neck cancer patients using FDG-PET imaging. In our study we predict that FDG-PET/CT will show potential in the evaluation of radiation-induced inflammation in the parotid gland that predisposes patients to xerostomia regardless of the radiation dose because we are focusing on the type of radiotherapy.

¹⁸F-fluorodeoxyglucose-positron emission tomography/computed tomography (FDG-PET/CT) is used in the clinical management of oncology and inflammatory pathologies. It may have utility in detecting RT-induced damage of oral tissues. In effort to confirm the correlation between FDG uptake, parotid gland inflammation, and saliva production. The aim of the present study is to demonstrate the feasibility of FDG-PET/CT in the detection and quantification of the inflammatory effect of RT on the parotid gland in HNC patients.

MATERIALS AND METHODS

Patient Population

Between 02/09/2010 and 11/27/2018, 64 patients with HNC treated with photon, proton, or combined photon/proton RT, in addition to chemotherapy with either cisplatin or cetuximab at the University of Pennsylvania. All patients were imaged pre- and 3 months post-treatment with FDG-PET/CT. Of the 64 patients, 17 were not included in the study due to technical issues associated with their FDG-PET/CT scans, inferior imaging quality in the head and neck region and/or mismatch between PET and CT

images. The collected clinical data included age, sex, and primary tumor location. The primary tumor locations were tongue, larynx, oropharynx, nasopharynx and hypopharynx. PET/CT scans used for the study were free from background noise, scatter, and metal artifacts. The study was approved by the Institutional Review Board. It was conducted in compliance with the Health Insurance Portability and Accountability Act (HIPAA).

FDG-PET/CT Image Acquisition

All subjects were injected intravenously with 5.0 MBq/kg FDG. After approximately 60 minutes FDG-PET/CT images were obtained using the same standardized protocol. Imaging was performed on hybrid PET/CT scanners with comparable spatial resolution (Siemens Biograph 64 mCT (Siemens Healthineers AG, Chicago, IL, USA) and Philips Gemini TF 16 (Philips Medical Systems, Andover, MA, USA)). The images were acquired in accordance with international guidelines[33,34] and the institutional PET/CT protocol, including quality control, calibration and harmonization of PET/CT scanners and validation of standardized uptake value (SUV) measurements. Patients fasted for at least 6 hours prior to scanning and serum glucose levels were immediately measured prior to FDG injection. Three acquisition protocols were used: one for body mass index (BMI) under 30, another for BMI between 30 and 35, and the third BMI over 35; the CT settings were 50, 100 and 150 mAs, respectively and all at 120 kVp. For the PET acquisitions, the time per bed was 1.5, 2, and 3 minutes, respectively. Low-dose CT imaging was performed for anatomic localization and attenuation correction. PET

images were corrected for scattering, attenuation, scanner dead time, and random coincidences.

FDG-PET/CT Image Analysis

FDG-PET/CT scans were analyzed using OsiriX MD software v.10.0.2 (DICOM viewer and image-analysis program, Pixmeo SARL; Bernex, Switzerland). Sequential axial PET/CT slices were used to draw regions of interest (ROI) manually around the right and left parotid glands using a closed polygon (**Figure 1**). The reader was blinded to the paired PET scans (pre- and post-treatment scans). Parotid gland ROIs were drawn beginning superiorly at the level of condyle down to the angle of the mandible inferiorly. The skin and external ear were defined as the lateral borders, the styloid process of the temporal bone was the medial border, and the mastoid process of the temporal bone was the posterior border.

The SUVmean was calculated as the average value of all voxels in the ROI. To determine the global activity of the parotid gland, the SUVmean as well as area (mm²) of each ROI at each transverse slice, was measured and recorded. The SUVmean was multiplied by the area, and the products were summed, the result of which was divided by the sum of the total area of the ROIs ($\text{Sum (SUVmean*Area)}/(\text{Sum Area})$). This resulted in the average SUVmean (Avg SUVmean) representative of a global inflammation burden of the parotid gland. The SUVmax was defined as the hottest voxel within the ROI. The average SUVmax (Avg SUVmax) represented the average value

from all trans-axial slices which include both right and left parotid glands. Statistical comparison was completed by using the Avg SUVmean and Avg SUVmax of all slices.

Statistical Analysis

For each subject, pre- and post-treatment Avg SUVmean and Avg SUVmax was calculated. A two-tailed paired t-test in STATA software (Stata/IC Version 10.1, StataCorp, College Station, TX) was used to compare the Avg SUVmean and Avg SUVmax in the pre- and post-treatment scans. The level of significance was defined as a p-value of less than 0.05. The average mean increases in SUVmean and SUVmax were calculated by subtracting pre-treatment from post-treatment Avg SUVmean and Avg SUVmax values for each patient.

RESULTS

The data collected from a total of 47 HNC patients (25 males, 22 females), mean age 59.7 years (range 42-78) with pre and post-treatment FDG-PET/CT were included. Thirty-three patients were in the photon RT group, while seven patients were in each of the proton RT and combined photon/proton RT groups. Primary tumor location, age, gender, and race are summarized in **Table 1**.

Statistical data are summarized in **Table 2 and 3**. The parotid gland Avg SUVmean in patients treated with photon RT was significantly higher in post-treatment scans (1.50, $p<0.05$) relative to those done pre-treatment (1.38, $p<0.05$) (**Figure 2**). The Avg

SUVmax was higher in post-treatment scans (2.06) compared to those done pre-treatment (1.96), but the difference was not statistically significant.

In patients treated with proton RT, the parotid gland Avg SUVmean was not significantly different in post-treatment scans (1.32, $p>0.05$) when compared to pre-treatment scans (1.25, $p>0.05$) (**Figure 3**). Evaluation of pre- and post-treatment scans for Avg SUVmax yielded a similar finding (post-treatment [1.73, $p>0.05$] and pre-treatment [1.72, $p>0.05$]).

Analysis of the parotid gland Avg SUVmean in patients treated with combined photon/proton RT was not significantly different in post-treatment scans (1.32, $p>0.05$) when compared to pre-treatment scans (1.25, $p>0.05$) (**Figure 4**). Similar findings were presented for Avg SUVmax (post-treatment [2.12, $p>0.05$] and pre-treatment [1.90, $p>0.05$]).

DISCUSSION

Our study demonstrates a significant increase in FDG uptake in the parotid glands of HNC patients following photon RT and chemotherapy treatments. Investigating the impact of these treatments on the parotid gland is critical, not only because of its role in saliva production but also due to the fact that cranial nerve VII (facial nerve) lies in close proximity to and innervates the gland. This nerve also innervates numerous muscles of facial expression, as well as the stylohyoid and posterior belly of the digastric muscles, which play a critical role in swallowing [20]. The glossopharyngeal nerve provides

parasympathetic innervation to the parotid gland, as well as sensory innervation to the posterior one-third of the tongue and pharynx. Photon RT and/or chemotherapy induced damage of the parotid gland can therefore impact glossopharyngeal nerve function and indirectly lead to deleterious effects on adjacent structures in the head and neck region [21]. Thus, determining the FDG uptake in the parotid gland is of clinical interest/importance in investigating potential previously underappreciated side effects of radiotherapy in head and neck cancer patients.

In our study, we found that Avg SUVmean was significantly higher in the parotid gland following photon RT, but not in patients who underwent proton RT or combined proton/photon RT. Although Avg SUVmean was significantly increased in patients receiving photon RT, SUVmax values were not significantly different in pre-treatment versus post-treatment scans of patients receiving any form of RT. SUVmax is the maximum voxel value of SUV in the target structure/ROI. SUVmax is simple and observer independent, hence SUVmax is the most commonly used parameter in clinical practice. However, SUVmax does not represent an entire structure's metabolic burden because the value is from only one voxel. Furthermore, SUVmax is sensitive to image noise, and is therefore impacted by various patient characteristics and imaging parameters. On the other hand, Avg SUVmean accounts for all uptake within the ROIs and is more reflective of the total pathological changes in glucose metabolism, which suggests that Avg SUVmean is a more accurate value to use in this data collection. Since we suspect that radiation-induced parotid injury is a diffuse pathology that has the potential to elicit an inflammatory response across the entire gland, we used the Avg

SUVmean as it is likely to be a more accurate indicator of the extent of the global inflammation.

There are several artifacts encountered in PET/CT imaging including attenuation correction artifacts commonly associated with the use of CT. Attenuation correction algorithms work well for most applications in the majority of patients. However, these algorithms tend to overcorrect objects that have higher density but are not true bone pixels. Dental implants or fillings can cause such an attenuation correction artifact and can confound image interpretation and effect the quantification in the head and neck region. In the present study, of the 64 patients, 17 were not included in the study due to technical issues including the presence of artifacts related to metallic based restorations, orthodontic appliances, and other dental procedures which are the main cause of beam hardening. This confirms the lack of beam hardening artifact effect on our measurements.

We assert that the increased FDG uptake observed in this study was a result of RT-induced inflammation in the parotid gland. Cellular uptake of FDG is a marker for inflammation, and these results confirm its utility in identifying parotid gland pathology following RT in head and neck cancer patients. In classic parotitis, this inflammation is most often the result of a localized infection or cellular damage, though the irritation can be caused by a myriad of factors, including pathogenic microbes derived from the oral cavity, metabolic imbalances, and autoimmune disorders [22]. Initiation of inflammatory processes in the gland can lead to a decrease in salivary production, causing

dehydration of the gland as well as a distortion of the parotid duct and metaplasia of the ductal epithelium [23]. Uptake of FDG may begin to increase subsequent to the preliminary irritation and continue to increase as the inflammatory response progresses [23]. Since RT has been shown to increase systemic inflammation, patients experience a significant risk in the perturbation of the parotid gland, since it is particularly susceptible to irritation [24,25].

It is critical to acknowledge the limitations of our study. This was a retrospective analysis with a relatively small sample size of patients. Thus, future evaluation of the use of FDG-PET/CT as a surrogate measurement of inflammatory activity in the parotid gland after RT treatment should be directed towards prospective studies using large numbers of patients. Information regarding full tumor stage, type of radiation field, the exact dosage of radiotherapy administered to patients, and oral complications were not available for the current study, which limited the description of our patient cohort. A survey reported that 64% of at least 3 years survivors after RT suffered from moderate to severe xerostomia [26]. Thus, future studies must include detailed information regarding the occurrence of xerostomia in order to determine whether increased parotid-uptake of FDG can be used to predict the onset of this condition. Partial volume effect, which accounts for signal overlap from neighboring anatomical structures and potential movement of the patients during scan acquisition, may have altered the data used in these analyses. Therefore, the regions used as borders in determining the extent of the ROIs may have been ambiguous, depending on the quality of the scan. The influence of partial volume effect is due to the limited resolution of the technology

used in obtaining these scans [27,28]. This could account for the single outlier observed in the data, which might have introduced further uncertainty into the results (**Figure 2**). In addition, because the patients who participated in the study received both chemotherapy and photon RT, it is not possible to differentiate between the inflammatory effects of each treatment individually. Finally, there were only two-time points assessed in this study, pre-treatment and 3 months post-treatment, which prevented the evaluation of FDG uptake throughout the entire post-treatment period.

The present study suggests that an increase beyond normal physiological glucose uptake in the parotid gland occurs as a manifestation of RT-induced inflammation. Given that inflammation is followed by cell damage and fibrosis of some of the glandular tissue [29], we predict that additional follow-up scans will demonstrate a decrease in the parotid gland uptake due to lack of normal gland activity and function. It would be helpful to direct future studies towards more longitudinal assessments of FDG uptake in the parotid gland to better track changes in signaling over time to determine the time frame of cell damage and fibrosis manifesting as a decline in parotid gland function compared to pre-treatment.

Protocols utilizing photon beams are currently the most common form of RT for HNC while less than 1% of patients are treated with proton therapy [30]. When comparing proton to photon therapy, proton therapy reveals an added advantage of lower dose and smaller number of beams [31]. In the present study, no significant differences were found between pre- and post-treatment parotid FDG uptake in patients treated with

proton RT. This observation might be indicative of there being less radiation delivered to normal tissues in close proximity to actual tumors thereby minimizing collateral toxicity and limiting the extent of side effects traditionally associated with photon-based RT [30,32].

The present study demonstrated significantly higher FDG uptake in the parotid glands of patients undergoing photon-based RT for treatment of HNC. This increase in glucose metabolism may be indicative of radiation-induced inflammation, which subsequently can progress result in decreased functionality of the parotid gland. Future studies should include a larger sample to allow comparison of the effect of photon RT for treatment of HNC to other modalities of RT in order to assess the differential impact on parotid gland function. Confirmation of the correlation between FDG uptake and saliva production might enable clinicians to choose alternative RT regimens and/or intervene at an earlier stage and prevent the sequela of xerostomia.

CONCLUSION

FDG-PET/CT has the potential to be used to measure the metabolic activity associated with RT-induced inflammation and predictor of parotid gland dysfunction.

LIST OF ABBREVIATIONS

- FDG-PET/CT: ¹⁸F-fluorodeoxyglucose-positron emission tomography/computed tomography.
- RT: radiotherapy.

- HNC: head and neck cancer.
- CT: computed tomography.
- MRI: magnetic resonance imaging.
- PET: positron emission tomography.
- FDG: ^{18}F -fluorodeoxyglucose.
- HIPAA: Health Insurance Portability and Accountability Act.
- SUV: standardized uptake value.
- Avg SUVmean: average mean standardized uptake value.
- Avg SUVmax: average maximum standardized uptake value.
- ROI: region of interest.
- BMI: body mass index.

DECLARATIONS

- Ethics approval and consent to participate:

Informed consent was obtained from all individual participants included in the study.

All procedures performed in studies involving human participants were in accordance with the ethical standards of the institutional and/or national research committee and with the 1964 Helsinki declaration and its later amendments or comparable ethical standards. The study was approved by the Institutional Review Board. It was conducted in compliance with the Health Insurance Portability and Accountability Act (HIPAA).

- Consent for publication: Not applicable.
- Availability of data and material:

All data generated or analyzed during this study are included in this article [and its supplementary information files].

- Competing interests:

The authors declare that they have no competing interests.

- Funding: Not applicable.

REFERENCES

- [1] Head and Neck Cancer - Statistics. CancerNet 2012.
<https://www.cancer.net/cancer-types/head-and-neck-cancer/statistics> (accessed November 9, 2019).
- [2] Alterio D, Marvaso G, Ferrari A, Volpe S, Orecchia R, Jereczek-Fossa BA. Modern radiotherapy for head and neck cancer. *Semin Oncol* 2019;46:233–45.
<https://doi.org/10.1053/j.seminoncol.2019.07.002>.
- [3] Giuranno L, Ient J, De Ruyscher D, Vooijs MA. Radiation-Induced Lung Injury (RILI). *Front Oncol* 2019;9:877. <https://doi.org/10.3389/fonc.2019.00877>.
- [4] Chrapko BE, Chrapko M, Nocun A, Stefaniak B, Zubilewicz T, Drop A. Role of 18F-FDG PET/CT in the diagnosis of inflammatory and infectious vascular disease. *Nucl Med Rev* 2016;19:28–36. <https://doi.org/10.5603/NMR.2016.0006>.
- [5] Chen S-C. Oral Dysfunction in Patients With Head and Neck Cancer: A Systematic Review. *J Nurs Res JNR* 2019;27:e58.
<https://doi.org/10.1097/jnr.0000000000000363>.
- [6] Shunmuga Sundaram C, Dhillon HM, Butow PN, Sundaresan P, Rutherford C. A systematic review of body image measures for people diagnosed with head and neck cancer (HNC). *Support Care Cancer* 2019;27:3657–66.
<https://doi.org/10.1007/s00520-019-04919-6>.
- [7] Dirix P, Nuyts S. Evidence-based organ-sparing radiotherapy in head and neck cancer. *Lancet Oncol* 2010;11:85–91. [https://doi.org/10.1016/S1470-2045\(09\)70231-1](https://doi.org/10.1016/S1470-2045(09)70231-1).
- [8] Mortazavi H, Baharvand M, Movahhedian A, Mohammadi M, Khodadoust A. Xerostomia due to systemic disease: a review of 20 conditions and mechanisms. *Ann Med Health Sci Res* 2014;4:503–10. <https://doi.org/10.4103/2141-9248.139284>.
- [9] Langendijk JA, Doornaert P, Verdonck-de Leeuw IM, Leemans CR, Aaronson NK, Slotman BJ. Impact of late treatment-related toxicity on quality of life among patients with head and neck cancer treated with radiotherapy. *J Clin Oncol Off J Am Soc Clin Oncol* 2008;26:3770–6. <https://doi.org/10.1200/JCO.2007.14.6647>.
- [10] Buchbender C, Heusner TA, Lauenstein TC, Bockisch A, Antoch G. Oncologic

- PET/MRI, part 1: tumors of the brain, head and neck, chest, abdomen, and pelvis. *J Nucl Med Off Publ Soc Nucl Med* 2012;53:928–38.
<https://doi.org/10.2967/jnumed.112.105338>.
- [11] Love C, Tomas MB, Tronco GG, Palestro CJ. FDG PET of Infection and Inflammation. *RadioGraphics* 2005;25:1357–68.
<https://doi.org/10.1148/rg.255045122>.
- [12] Rege SD, Chaiken L, Hoh CK, Choi Y, Lufkin R, Anzai Y, et al. Change induced by radiation therapy in FDG uptake in normal and malignant structures of the head and neck: quantitation with PET. *Radiology* 1993;189:807–12.
<https://doi.org/10.1148/radiology.189.3.8234708>.
- [13] Fletcher JW, Djulbegovic B, Soares HP, Siegel BA, Lowe VJ, Lyman GH, et al. Recommendations on the Use of 18F-FDG PET in Oncology. *J Nucl Med* 2008;49:480–508. <https://doi.org/10.2967/jnumed.107.047787>.
- [14] Beichel RR, Ulrich EJ, Smith BJ, Bauer C, Brown B, Casavant T, et al. FDG PET based prediction of response in head and neck cancer treatment: Assessment of new quantitative imaging features. *PLoS ONE* 2019;14.
<https://doi.org/10.1371/journal.pone.0215465>.
- [15] Castaldi P, Leccisotti L, Bussu F, Micciché F, Rufini V. Role of (18)F-FDG PET-CT in head and neck squamous cell carcinoma. *Acta Otorhinolaryngol Ital Organo Uff Della Soc Ital Otorinolaringol E Chir Cerv-Facc* 2013;33:1–8.
- [16] Baumann BC, Mitra N, Harton JG, Xiao Y, Wojcieszynski AP, Gabriel PE, et al. Comparative Effectiveness of Proton vs Photon Therapy as Part of Concurrent Chemoradiotherapy for Locally Advanced Cancer. *JAMA Oncol* 2020;6:237–46.
<https://doi.org/10.1001/jamaoncol.2019.4889>.
- [17] Grant SR, Grosshans DR, Bilton SD, Garcia JA, Amin M, Chambers MS, et al. Proton versus conventional radiotherapy for pediatric salivary gland tumors: Acute toxicity and dosimetric characteristics. *Radiother Oncol* 2015;116:309–15.
<https://doi.org/10.1016/j.radonc.2015.07.022>.
- [18] Ramaekers BLT, Pijls-Johannesma M, Joore MA, Ende P van den, Langendijk JA, Lambin P, et al. Systematic review and meta-analysis of radiotherapy in various head and neck cancers: Comparing photons, carbon-ions and protons. *Cancer*

- Treat Rev 2011;37:185–201. <https://doi.org/10.1016/j.ctrv.2010.08.004>.
- [19] Roach MC, Turkington TG, Higgins KA, Hawk TC, Hoang JK, Brizel DM. FDG-PET assessment of the effect of head and neck radiotherapy on parotid gland glucose metabolism. *Int J Radiat Oncol Biol Phys* 2012;82:321–6. <https://doi.org/10.1016/j.ijrobp.2010.08.055>.
- [20] Dulak D, Naqvi IA. *Neuroanatomy, Cranial Nerve 7 (Facial)*. StatPearls, Treasure Island (FL): StatPearls Publishing; 2019.
- [21] García Santos JM, Sánchez Jiménez S, Tovar Pérez M, Moreno Cascales M, Lailhacar Marty J, Fernández-Villacañas Marín MA. Tracking the glossopharyngeal nerve pathway through anatomical references in cross-sectional imaging techniques: a pictorial review. *Insights Imaging* 2018;9:559–69. <https://doi.org/10.1007/s13244-018-0630-5>.
- [22] Patel P, Scott S, Cunningham S. Challenging Case of Parotitis: A Comprehensive Approach. *J Am Osteopath Assoc* 2017;117:e137–40. <https://doi.org/10.7556/jaoa.2017.152>.
- [23] Chitre VV, Premchandra DJ. Recurrent parotitis. *Arch Dis Child* 1997;77:359–63. <https://doi.org/10.1136/ad.77.4.359>.
- [24] Brook I. Diagnosis and Management of Parotitis. *Arch Otolaryngol Neck Surg* 1992;118:469–71. <https://doi.org/10.1001/archotol.1992.01880050015002>.
- [25] Schae D, Micewicz ED, Ratikan JA, Xie MW, Cheng G, McBride WH. Radiation & Inflammation. *Semin Radiat Oncol* 2015;25:4–10. <https://doi.org/10.1016/j.semradonc.2014.07.007>.
- [26] Wijers OB, Levendag PC, Braaksma MMJ, Boonzaaijer M, Visch LL, Schmitz PIM. Patients with head and neck cancer cured by radiation therapy: a survey of the dry mouth syndrome in long-term survivors. *Head Neck* 2002;24:737–47. <https://doi.org/10.1002/hed.10129>.
- [27] Cysouw MCF, Kramer GM, Hoekstra OS, Frings V, de Langen AJ, Smit EF, et al. Accuracy and Precision of Partial-Volume Correction in Oncological PET/CT Studies. *J Nucl Med Off Publ Soc Nucl Med* 2016;57:1642–9. <https://doi.org/10.2967/jnumed.116.173831>.
- [28] Soret M, Bacharach SL, Buvat I. Partial-Volume Effect in PET Tumor Imaging. *J*

Nucl Med 2007;48:932–45.

- [29] Wynn TA, Ramalingam TR. Mechanisms of fibrosis: therapeutic translation for fibrotic disease. *Nat Med* 2012;18:1028–40. <https://doi.org/10.1038/nm.2807>.
- [30] Mohan R, Grosshans D. Proton therapy - Present and future. *Adv Drug Deliv Rev* 2017;109:26–44. <https://doi.org/10.1016/j.addr.2016.11.006>.
- [31] Levin WP, Kooy H, Loeffler JS, DeLaney TF. Proton beam therapy. *Br J Cancer* 2005;93:849–54. <https://doi.org/10.1038/sj.bjc.6602754>.
- [32] Lin A, Swisher-McClure S, Millar LB, Kirk M, Yeager C, Kassaei A, et al. Proton therapy for head and neck cancer: current applications and future directions. *Transl Cancer Res* 2012;1:255-263–263. <https://doi.org/10.21037/786>.
- [33] Delbeke D, Coleman RE, Guiberteau MJ, Brown ML, Royal HD, Siegel BA, et al. Procedure Guideline for Tumor Imaging with 18F-FDG PET/CT 1.0. *J Nucl Med* 2006;47:885–95.
- [34] Boellaard R, Delgado-Bolton R, Oyen WJG, Giammarile F, Tatsch K, Eschner W, et al. FDG PET/CT: EANM procedure guidelines for tumour imaging: version 2.0. *Eur J Nucl Med Mol Imaging* 2015;42:328–54. <https://doi.org/10.1007/s00259-014-2961-x>.

Table 1. Primary tumor location, age, gender, and race.

Primary Tumor Location	Number of Patients		Average Age (Years)	Race		
	Males	Females		White	African American	Other
Tongue	14	3	61.97	15	2	0
Larynx	3	2	54.66	4	0	1
Oropharynx	3	14	58.70	13	3	1
Nasopharynx	3	2	58.25	3	1	1
Hypopharynx	2	1	62.73	2	0	1

Table 2. Parotid gland average mean standardized uptake value (Avg SUVmean) and in head-and-neck cancer patients pre- and post-treatment scans.

Avg SUVmean (g/mL)	Pre-treatment	Post-treatment	P-value
Photon Therapy	1.38	1.50	0.03
Proton Therapy	1.25	1.32	0.31
Combined Therapy	1.51	1.46	0.40

Table 3. Parotid gland average maximum standardized uptake value (Avg SUVmax) and in head-and-neck cancer patients pre- and post-treatment scans.

Avg SUVmax (g/mL)	Pre-treatment	Post-treatment	P-value
Photon Therapy	1.96	2.06	0.18
Proton Therapy	1.72	1.73	0.50
Combined Therapy	1.90	2.12	0.21

Figure 1. ^{18}F -fluorodeoxyglucose positron emission tomography/computed tomography (FDG-PET/CT) images of the parotid gland. Left: Fused FDG PET/CT, right: CT. The delineation of the region of interest (ROI) is highlighted for the right and left parotid glands.

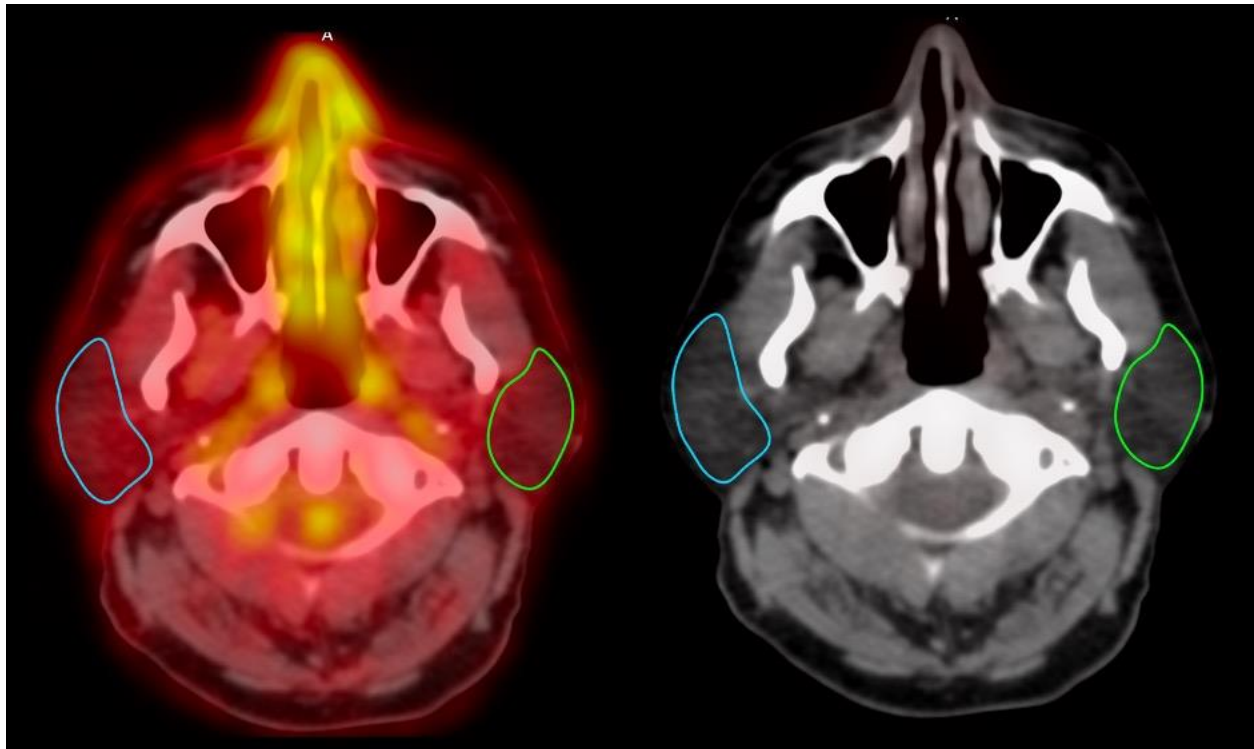


Figure 2. Changes in average standardized uptake value mean (Avg SUVmean) of the parotid gland before and 3 months after treatment in patients treated with photon RT.

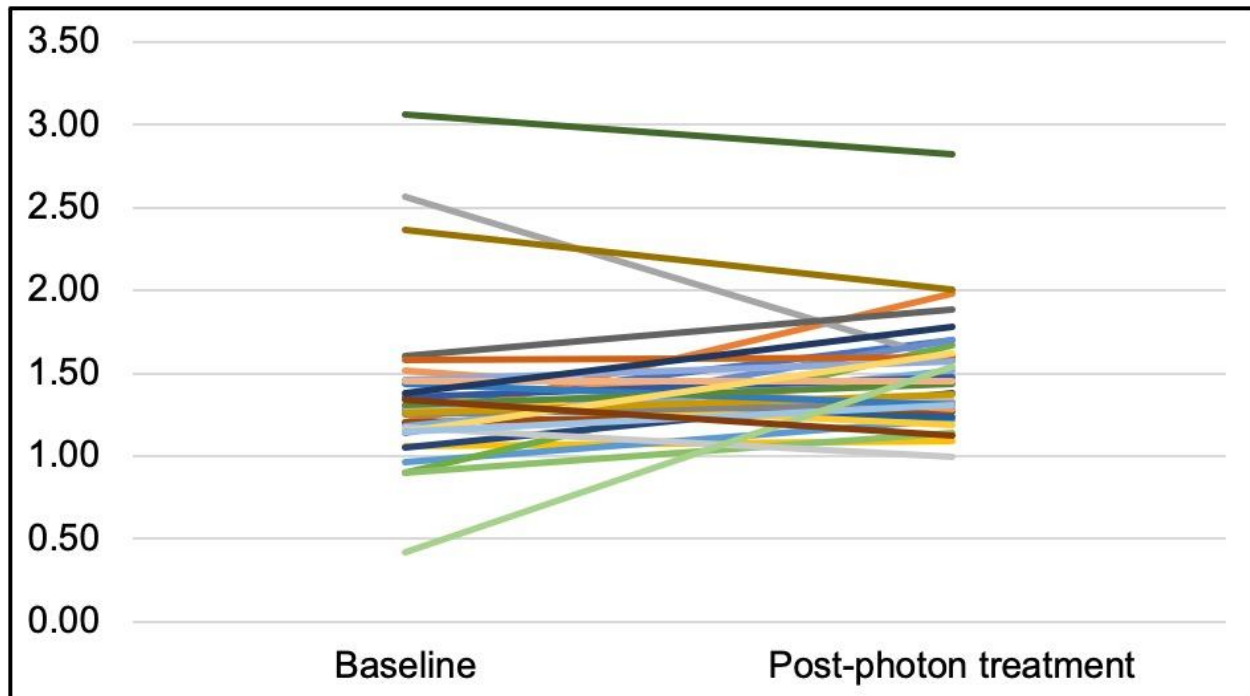


Figure 3. Changes in average standardized uptake value mean (Avg SUVmean) of the parotid gland before and 3 months after treatment in patients treated with proton RT.

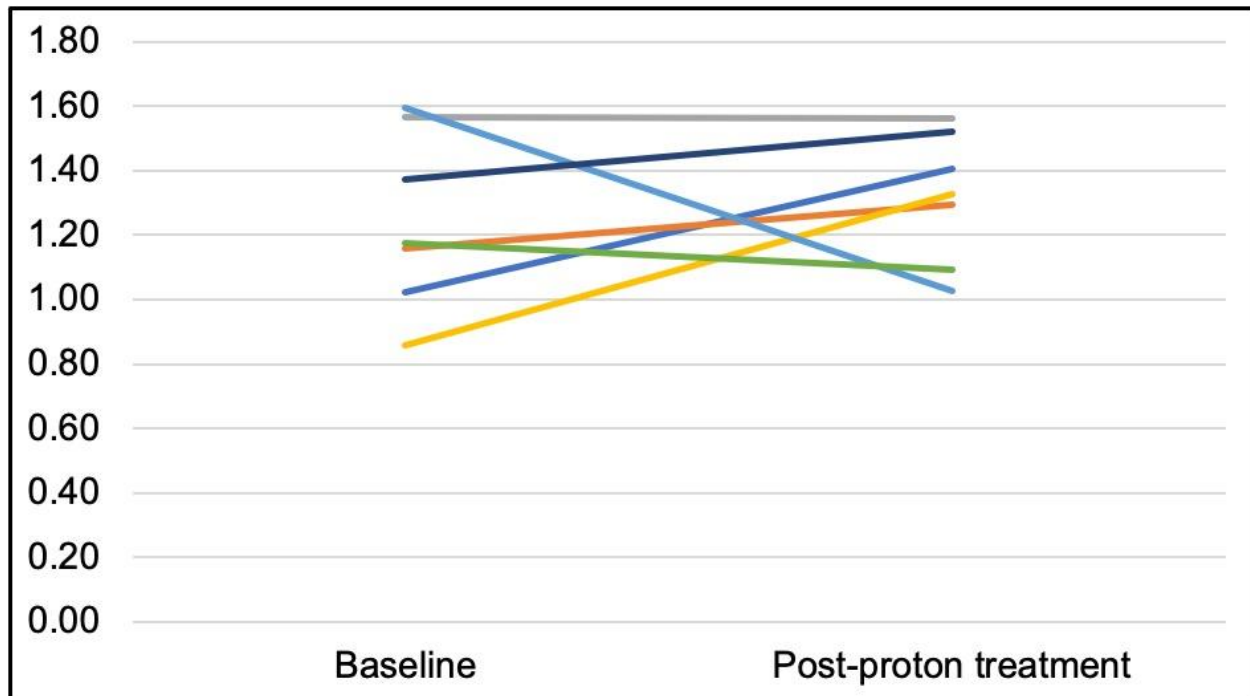


Figure 4. Changes in average standardized uptake value mean (Avg SUVmean) of the parotid gland before and 3 months after treatment in patients treated with combined photon/proton RT.

